Molecular Fluid Flow in MoS_2 Nanoporous Membranes and Hydrodynamics Interactions

João P. K. Abal[1, a)] and Marcia C. Barbosa[1, b)]
[1]*Institute of Physics, Federal University of Rio Grande do Sul, 91501-970, Porto Alegre, Brazil*

(Dated: 11 March 2021)

We study the impact of the induced pressure fields in the water flow and salt rejection in nanopores produced in MoS_2 membranes. We observe that the water permeability and the salt rejection are not impacted by the distance between the pores. This result contradicts the continuous fluid mechanics calculations in microfilters which indicates the existence of hydrodynamic interactions between adjacent pores which increase the water mobility. Our results suggests that at this nanoscale the hydrodynamic interactions does not affect the water mobility through nanopores.

Keywords: Desalination, Nanoporous Membrane, Hydrodynamic Interactions, Nanofluidics, Molecular Dynamics, Water, 2D membrane, MoS_2

I. INTRODUCTION

Water scarcity is one of the major challenges of our time. Changing climate patterns responsible for disturbing the hydrological cycle combined with growing water demand are shifting the water security towards high-risk levels[1]. In the face of the problem, seawater desalination technology has gained attention. Over the past decades, improvements in the sector have allowed a considerable reduction of power needed to desalinate seawater, due to advances in membrane technology and energy recovery equipment[2,3].

High-performance membranes, that can exhibit superior selectivity and high water flowrate are key to the next-generation desalination technology[3,4]. Meanwhile, computational models have been used to better understand the desalination process at the nanoscale. In this context, molecular dynamics simulations are a powerful theoretical approach to study the physics behind nanofluidic systems once it allows for probing the microscopic behavior of a collection of atoms while performing timescale feasible simulations[5,6], giving rise to new membrane materials nanostructured designed to improve the desalination process.

One suited simulation branch to better understand the desalination process is mimic the reverse osmosis desalination system at the nanoscale[8–20]. This technique enters in the scope of Non-Equilibrium Molecular Dynamics (NEMD). Also, its procedure has been used to get insights in design new membrane materials for desalination. Recently a number of studies suggest molybdenum disulfide (MoS_2) as a promising nanoporous membrane not only due to its water permeability but also for its salt selectivity[16,17,21–26].

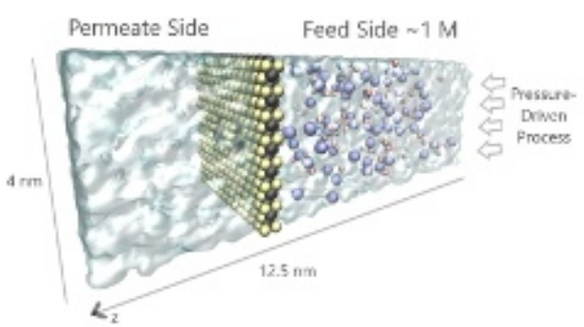

FIG. 1. The illustration of a typical NEMD desalination system at the nanoscale. The saltwater (right side) is separated from the pure water (left side) by a MoS_2 nanoporous membrane. Pressure-driven transport can be simulated by imitating the reverse osmosis process. Image created using the VMD software[7].

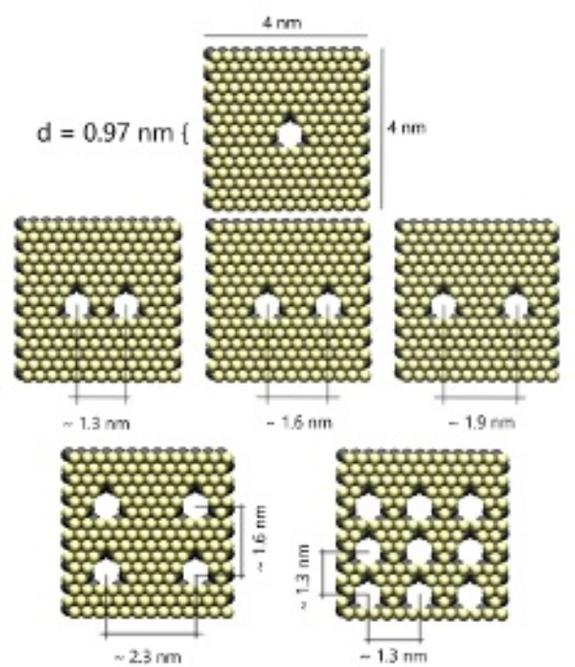

FIG. 2. The MoS_2 nanoporous membranes studied in this work. All the membranes are square shaped (4x4nm).

a)Electronic mail: joao.abal@ufrgs.br
b)Electronic mail: marcia.barbosa@ufrgs.br

The transport properties of water confined in nanopores are very different from the bulk water and are not properly described by the continuum hydrodynamics[27]. The continuum hypothesis is one of the fundamentals assumptions of fluid mechanics, which is successful in describing the macroscopic behavior of fluid flow and states that fluid properties, such as pressure, density, and velocity, are well defined at infinitesimally small points and vary continuously from one point to another[28]. However, in narrow nanopores (< 2 nm of diameter), the water flow is layered and a non-quadratic velocity profile emerges from it[29]. For such small molecular size pores, the hydrodynamics approach fails. Then, it is more useful to discuss the fluid transport using permeability and flow rate rather than viscosity and slip length, for example[28].

The continuous fluid mechanics calculations in microfilters assumes the existence of hydrodynamic interactions between adjacent pores. The interaction arises from the pressure field induced by the next pore which in turn makes the single pore water flow solution not sufficiently precise to expand its conclusions to the microfilters flow system[30]. The influence of the pore number and its distance plays an important role in the overall water flux in the classical hydrodynamic picture. Ignoring these pore-pore "interaction", the simulations conducted so far in the scope of molecular dynamics desalination systems assume that the water flux results scale linearly with the nanopore number[31] in an "ideal gas" modeling of the system.

In this work we test if the assumption that the distance between identical pores does not affect the transport properties of water in a nanopore membrane is valid. We employ NEMD simulations to investigate the behavior of liquids in the nanoscale[32]. We obtain the nanopore number and its proximity implications in water flux and salt rejection. We use six different MoS_2 membrane (crystal structure of 2H) designs with different nanopore number and different nanopore distance (Figure 2). These membranes were designed in order to maintain the nanopore chemistry and geometry the same in each case. So, the only difference in water flow would be due to hydrodynamic interactions. The remaining of the paper goes as follows. In chapter II the computation details are presented and the results are commented in chapter III. The conclusions follows the chapter IV.

II. COMPUTATIONAL DETAILS

Our system is designed as two reservoirs, one with water and salt molecules, the feed side, and another with only pure water, the permeate side. The two reservoirs are separated by a membrane, as illustrated in Figure 1. The system is limited in the z direction by graphene barriers which in turn can serve as pistons to control the fluid pressure during the running desalination process. We analyze six systems with pore diameter of 0.97nm: one single pore at the center of the membrane, three pairs of pores separated by 1.3 nm,1.6 nm and 1.9 nm, four and nine pores, as illustrated in Figure 2.

TABLE I. The Lennard-Jones parameters and atoms charges employed in the simulations.

	σ_{LJ} [Å]	ε_{LJ} [kcal/mol]	Charge (e)
Na[33]	2.52	0.0346	0.885
Cl[33]	3.85	0.3824	-0.885
O-Tip4p/ε[34]	3.165	0.1848	-1.054
H-Tip4p/ε[34]	0.0	0.0	0.5270
Mo[35]	4.20	0.0135	0.6
S[35]	3.13	0.4612	-0.3
C[36]	3.40	0.0860	0.0

The system is initialized with 1550 water molecules at the permeate side and 170 ions mixed with 4930 water molecules at the feed side, resulting in a solution of 1 mol/L of concentration. The MoS_2 membrane has a dimension of 4 x 4 nm and it is held fixed in space. We work with high gradient pressures for statistical purposes, allowing us to generate a large number of events in a time interval of 10 ns. The MoS_2 has nanopores with 0.97 nm in diameter (defined as the distance center to center of atoms) what is the minimum size which does not show the ion blockage effect[18].

The simulations were performed using the LAMMPS[37]. The particles interact with each other via Lennard-Jones (LJ) and Coulomb potentials. The parameters used in this work are summarized in Table I. The Tip4p/ε water and NaCl/ε models were selected because they provide the correct value of bulk water[34] and water-NaCl[33] dielectric constants important for our analysis.

The simulations were performed as follows. First, the nanopore was kept closed and the two reservoir were isolated. We performed simulations during 0.5 ns in the NVE ensemble. Next, simulations were conducted in the NPT ensemble during 1 ns at 300 K and 1 bar at each reservoir. Then, the simulation was further equilibrated for 2 ns at 300 K in NVT ensemble to achieve the water equilibrium density of 1 g/cm^3. Finally, the nanopore was opened by removing the desired atoms from the MoS_2 sheet and the different pressures were applied at each reservoir for 10 ns. The feed pressures used in this work were from 100, 500, 1000, 2500, 5000 to 10000 bars.

The water flux throughout the membrane is computed by the membrane specific permeability[31], namely

$$A_m = \frac{\phi}{(P-\Pi)} \tag{1}$$

which incorporates information about the nanopore density and the membrane resistance to water flow (the pressure needed to induce certain flow). In this expression ϕ is the water flux, P is the applied pressure and Π is the osmotic pressure, and has dimensions of $L/m^2/hr/bar$ or LMH/bar.

III. RESULTS

In order to test if the water flow through nanopores in MoS_2 membranes obey the hydrodynamic behavior, we compare the

flow of a single pore, two pores at three distances, four and nine pores. Classical hydrodynamics predicts that for pores close enough the behavior is not the same observed in a single pore[30]. First, we analyze the membrane permeability. Figure 3 illustrates the membrane permeability as a function of pressure for six cases: isolated pore, two pores separated by 1.3 nm, 1.6 nm and by 1.9 nm, four and nine pores. The graph shows that the membrane permeability is a linear function of the gradient pressure. Using Eq. 1 we obtained the specific permeability as illustrated in Table II.

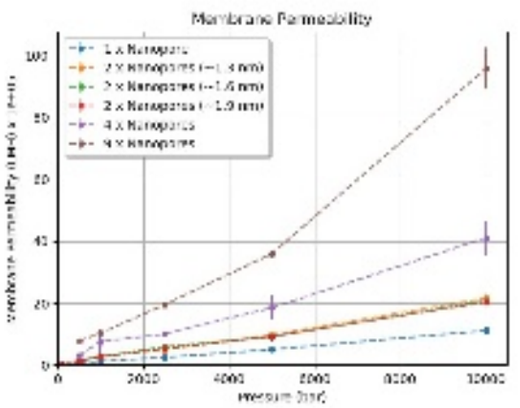

FIG. 3. The membrane permeability as a function of pressure for each membrane design. The error bars are the deviation from the mean value (errors bars smaller than the points are not shown).

TABLE II. The membrane specific permeabilities (A_m) obtained as function of nanopore density and distance. The numbers inside the parentheses are the membrane specific permeabilities standard deviations evaluated in this work.

Nanopore Density [10^{12} cm^{-2}]	A_m [LMH/bar]	Distance [nm]
1 x Nanopore - 6.25	101.7 (25.2)	
2 x Nanopores - 12.5	242.9 (55.8)	1.3
2 x Nanopores - 12.5	241.6 (54.7)	1.6
2 x Nanopores - 12.5	223.6 (38.1)	1.9
4 x Nanopores - 25.0	436.0 (87.1)	2.3x1.6
9 x Nanopores - 56.25	934.2 (323)	1.3x1.3

Next, we study the behavior of the salt in the analyzed configurations. In reverse osmosis an efficient system is expect to show a salt rejection higher than 99%[2]. Figure 4 shows that the MoS_2 nanoporous membrane with 0.97nm of diameter exhibits an excellent salt rejection capability, achieving 100% of rejection per pore working in pressures below 1000 bar. The graph also shows that the salt rejection per nanopore not only is the same for one or more pores but also does not depend on the distance between the pores.

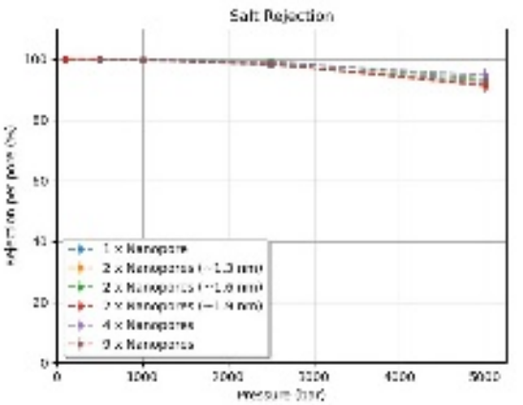

FIG. 4. The salt rejection per nanopore as function of pressure. The error bars are the deviation from the mean value. For small pressure gradients (< 100 bars), near from the realistic process operation in reverse osmosis systems[19], the salt rejection is 100% for such MoS_2 nanopore size.

Another important aspect of the reverse osmosis process is the concentration polarization (CP) phenomena, which is responsible to reduce the water flux due to increased local osmotic pressure near the membrane, namely the accumulation of salt near the membrane surface. Although the CP implications are higher for high water flow rates in reverse osmosis systems, this effect is observed within dozens of μm from the membrane surface[38]. Our nanoscale simulation box is too small to capture this effect, as we can see from the constancy of the salt concentration along the z-direction shown in Figure 5.

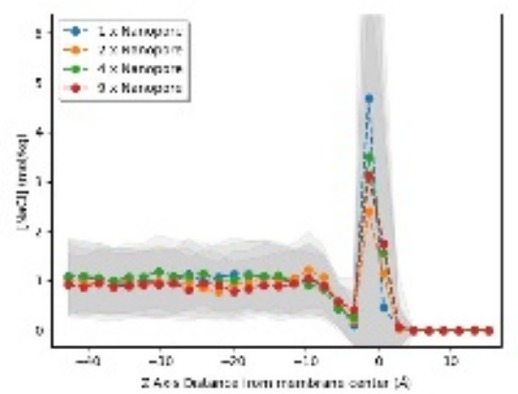

FIG. 5. The salt concentration along the simulation box in z-direction from membrane center. The shadows represents the concentration standard deviation during the running process.

Then we studied the water flow rate per pore. The permeability per pore is the same in all cases, as the pores approach no decrease of the permeability is observed, as we can see from Figure 6.

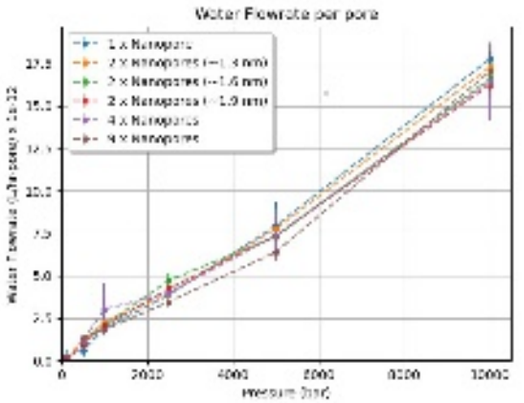

FIG. 6. Water flowrate per pore as a function of applied pressure.

In Figure 7 the membrane specific permeability as a function of membrane porosity is shown. The area of the so-called 0.97nm diameter pore corresponds to 0.66nm^2. Here we added a new nanopore design for hydrodynamic resistance comparison: a single nanopore with 1.33nm of diameter corresponding to an area of 1.19nm^2. The pore area was obtained by computing the accessible area to water molecules considering the size of the atoms on the edge of the pore as the van der Waals radii of sulfur and molybdenum. We found that in this scale the membrane specific permeability increases linearly, within the error bars, with membrane porosity for the 0.97nm diameter systems.

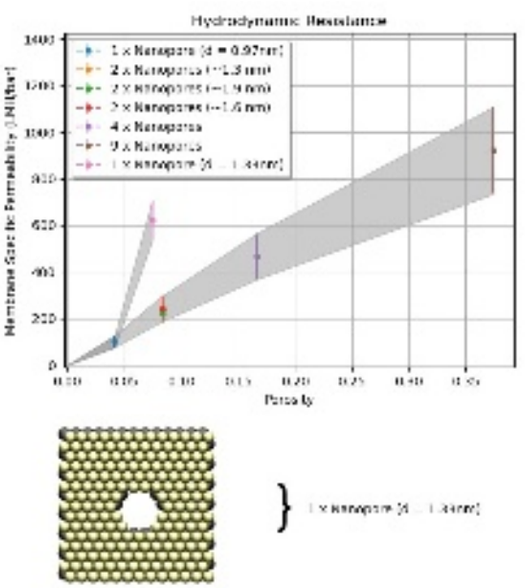

FIG. 7. Hydrodynamic resistance as membrane specific permeability versus membrane porosity. Beyond the set of nanopores with 0.97nm of diameter investigated in this work, here we show a comparison with a single nanopore with 1.33nm of diameter in order to illustrate the difference in hydrodynamic resistance.

These results reinforce the fact that the hydrodynamic interactions between adjacent pores do not play a significant role in this scale. Besides that, the large nanopore, named (1 x Nanopore (d = 1.33nm)), represents another set of hydrodynamic resistance, as shown in Figure 7. It is worth to mention the 1.33nm diameter nanopore shows a higher water flow rate for the same porosity at the cost of lower salt rejection performance. As mentioned before, the whole set of 0.97nm nanopores has 100% of salt rejection for small pressure gradients (< 1000 bars as shown in Figure 4), while the 1.33nm of diameter nanopore shows 97% of salt rejection at the same pressure. This is the trade-off between selectivity and permeability that we have to deal with.

Then, in order to investigate if the membrane permeability is independent of the number of pores by a compensation of effects, we tested what happens with the mobility of water through the membrane in the four cases: the one single pore versus the three pairs of pores separated by 1.3 nm, 1.6 nm and 1.9 nm. Water flux, Q, is a function of the water density inside the pore channel, ρ, the velocity, v, and the pore area, A, namely

$$Q = \rho \cdot v \cdot A \, . \tag{2}$$

The area A of the pores is a geometric parameter that, in turn, is maintained constant in our simulations. The density, ρ, and the axial velocity, v, are the remaining control parameters and they are related to the pore chemistry[5,16,17]. The pore chemistry depends on the particle interactions and their distribution around the pore. We know from previous studies that the charge distribution affects the overall water flux[39–41]. In our simulations, we chose an arrangement of atoms, as illustrated in Figure 2, to maintain constant the proportion between hydrophobic and hydrophilic sites in the pore. As a consequence of this choice, the charge distribution is the same in each one of the four cases and the pores are charge neutral. In summary, the nanopore chemistry and geometry are the same in all simulations. By doing that, we expect that any change in the water flux as a function of nanopore number or distance would be due to hydrodynamics interactions between the pores, which in turn would be reflected in the water flux or water density around the pores[30].

Figure 6 shows the water flowrate per pore in the six cases. The graph indicates that there is no dependence of the flow on the nanopore number or on the distance between the pores. This result indicates that the classical hydrodynamic predictions fail in the systems we analyzed. The classical hydrodynamic equations assume the fluid distribution to be continuum what is not the case. In order to confirm that the dynamics of water is localized and not continuum, we investigate the water density inside and around the pore. Oxygen distribution of water is illustrated in Figure 8. The *Region 1* is defined as the water present between 8 > z > 3 Å where z is the distance from the membrane center (Mo atoms) and the positive numbers correspond to the permeate side. The *Region 2* corresponds to 3 > z > 1.56 Å and the *Region 3* is the water located at 1.56 > z > -1.56 Å (the nanopore region).

The oxygen color map illustrated in Figure 9-*Region 3* shows how the water moves through the single and double

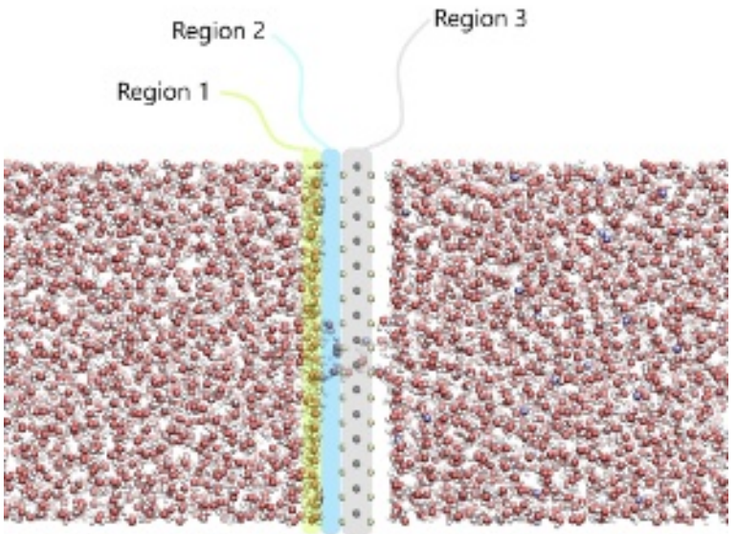

FIG. 8. Oxygen distribution of water in the two side of the membranes. The three different *Region 1*, *Region 2* and *Region 3* are indicated by yellow, blue and gray respectively.

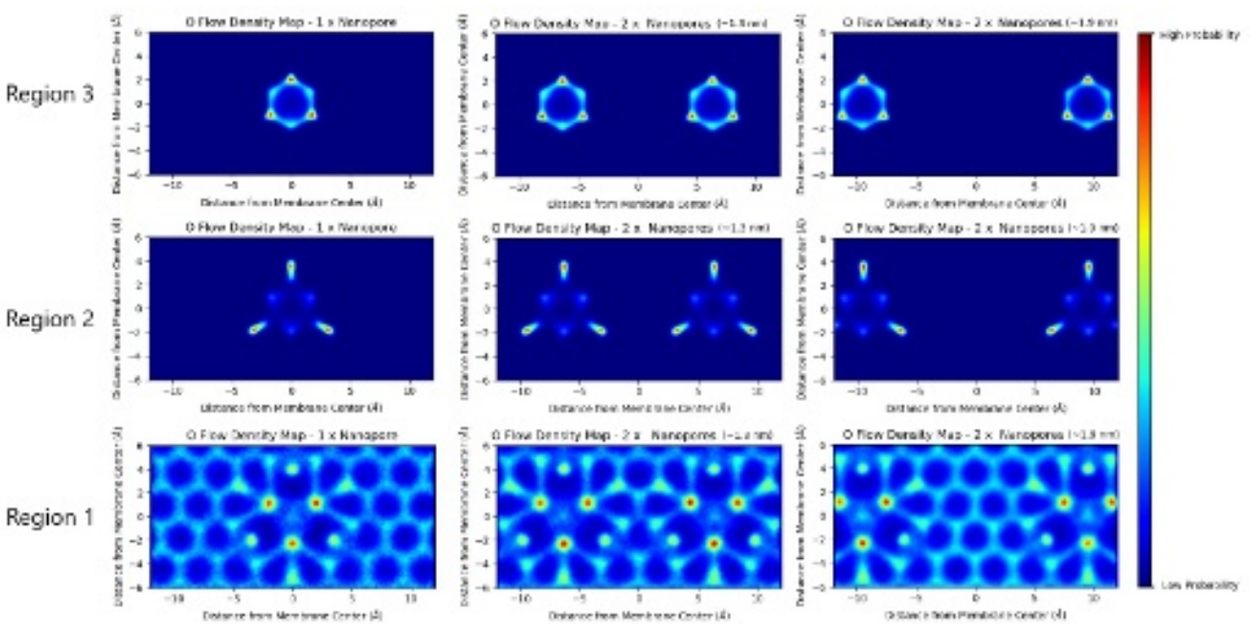

FIG. 9. Oxygen color map indicating as red the high density, light blue as low density and dark blue absence of water.

nanopores. The three maps for this *Region 3* show that the water molecules transport inside the pore occurs near the Mo atoms at the pore surface and the water does not pass throughout the pore center. Layered water structure, described by density oscillations in the radial direction, arises and it is a signature of the implications of nanoconfinement. Figure 9-*Region 2* shows that water molecules enter in the nanopore attracted mostly by the Mo sites[16]. In addition, the first two water layers from the membrane surface shown in Figure 9-*Region 1* indicate that even in this layer outside the pore, molecules prefer to stay between S sites, which is the region in which the Mo-water electrostatic interaction is less screened by the S atoms.

The oxygen density map from Figure 9-*Region 1* in the single nanopore case (left column) shows that the first two water layers are modified locally by the presence of the nanopore. However, its extension is not larger than the nanopore size of 0.97 nm of diameter, which suggests that the nanopore presence does not have a large effect in the water structure near the membrane, just local implications near the nanopore region.

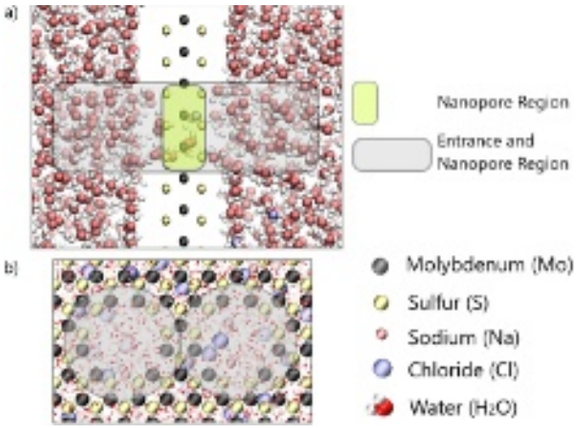

FIG. 10. a) The definitions of nanopore region and entrance region for the water density analysis. b) The front view of the cylindrical regions of analysis.

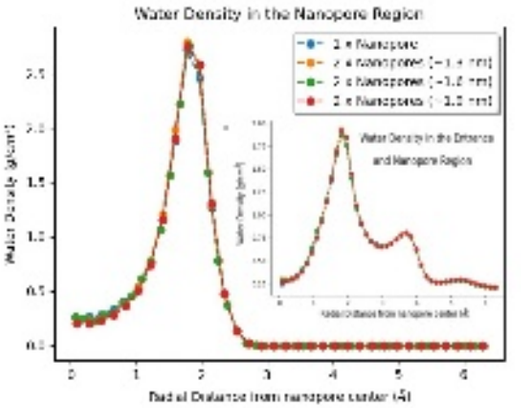

FIG. 11. The water density as a function of radial distance from each nanopore center in the nanopore region. In the detail: The water density as a function of radial distance from each nanopore center in the entrance and nanopore region.

Comparing with the two neighboring nanopores case, no deviation in the density map due to the presence of the second nanopore is observed. This conclusion extends to the last case, when the two nanopores have the larger separation. To quantify if any implications in the water density exist due to the proximity of nanopores, we obtained the water density as a function of the radial distance from each nanopore center, as defined in Figure 10. The radial water density was calculated binning the region inside the nanopore in circular shapes, counting the water molecules there, and dividing by its cylindrical volume.

As we can see from Figure 11 there is no difference in the water density inside the nanopore due to the presence of a second one. Figure 11 shows that if any induced pressure field extends from one nanopore to the other one, it is not sufficient to produce a change in the water density inside the nanopore and its surroundings.

In addition, the water density is related to the Potential of Mean Force (PMF) through the following expression[17,25,42]

$$PMF(z) = -k_b T ln[\rho(z)/\rho_0] \, . \tag{3}$$

where $\rho(z)$ is the local density, the ρ_0 is the bulk density, T is the temperature and k_b is the Boltzmann constant. The Eq. 3 is usually computed in equilibrium states. However, we extrapolated the calculations to the steady-state flow once it refers to states near equilibrium, and our goal is to catch dynamic features.

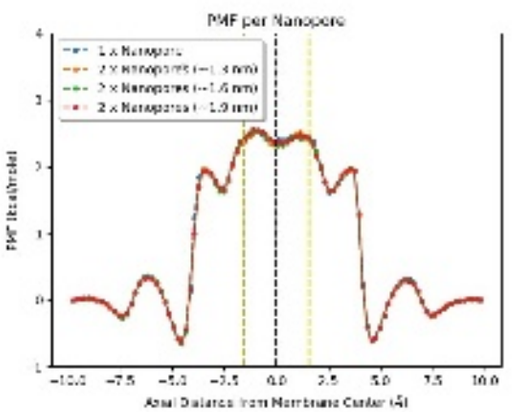

FIG. 12. The water PMF per nanopore as a function of axial distance from the membrane. The dashed lines represent the Sulfur layer (yellow line) and the Molybdenum layer (black line).

The free energy barrier ΔG can be established from Figure 12 and it is related to the probability of water molecules been able to overcome the nanopore energy barrier $P \sim exp(\Delta G/k_b T)$. As it can be seen, the PMF per nanopore is the same for each membrane. The hydrodynamic effects were not visible in this scale may be due to the polar nature (atomic charges) of the MoS_2 membrane, which induces its structure in the first water layer[26].

IV. CONCLUSIONS

Differently from the classical fluid mechanics calculations in microfilters[30], the fluid flow through neighboring nanopores in MoS_2 membranes does not show in our NEMD simulations any significant hydrodynamic interactions between adjacent pores. The water flow strongly depends on the

intermolecular force of the membrane, which is governed by the layered structure of the liquid in the nanopore region, and as a consequence, the collective effect of hydrodynamic interaction between pores is suppressed. Nevertheless, we shed light on the assumption that the water flux would scale linearly with the nanopore density regardless of its distance. Of course, here the MoS_2 atoms were held fixed in space, and more careful simulations are needed to understand the relation between nanopores distance and material stability. Based on the results of Cohen-Tanuji et. al.[19], although higher pressures gradient leads to greater membrane deformation, the implications of that are not significant to the flow of water across the graphene nanopores. Since MoS_2 monolayer has effective Young's modulus[43] of $180 \pm 60\ Nm^{-1}$ while graphene[43] has $335\ Nm^{-1}$, we expect the main conclusions of our work would not be affected if flexibility would be taken into account. As previous studies confirmed, the MoS_2 nanoporous membranes are promising candidates for the next-generation membrane material, allowing water to be filtered at high permeate rates while maintaining high salt rejection rates for sufficiently narrow pores.

ACKNOWLEDGEMENTS

This work is financially supported by the Brazilian agency CNPq. We thank the CENAPAD/SP and CESUP/UFRGS for the computer time.

AVAILABILITY OF DATA

The data that support the findings of this study are available from the corresponding author upon reasonable request.

[1] U. W. W. A. Programme, "Water and climate change," The United Nations world water development report 2020 (2020).
[2] N. Voutchkov, "Energy use for membrane seawater desalination – current status and trends," Desalination **431**, 2 – 14 (2018).
[3] P. J. J. Alvarez, C. K. Chan, M. Elimelech, N. J. Halas, and D. Villagrán, "Emerging opportunities for nanotechnology to enhance water security," Nature Nanotechnology **13**, 634–641 (2018).
[4] J. R. Werber, C. O. Osuji, and M. Elimelech, "Materials for next-generation desalination and water purification membranes," Nature Reviews Materials **1**, 16018 (2016).
[5] D. Cohen-Tanugi and J. C. Grossman, "Nanoporous graphene as a reverse osmosis membrane: Recent insights from theory and simulation," Desalination **366**, 59 – 70 (2015), energy and Desalination.
[6] E. R. Smith, "A molecular dynamics simulation of the turbulent couette minimal flow unit," Physics of Fluids **27**, 115105 (2015), https://doi.org/10.1063/1.4935213.
[7] W. Humphrey, A. Dalke, and K. Schulten, "VMD – Visual Molecular Dynamics," Journal of Molecular Graphics **14**, 33–38 (1996).
[8] C. Zhu, H. Li, and S. Meng, "Transport behavior of water molecules through two-dimensional nanopores," The Journal of Chemical Physics **141**, 18C528 (2014), https://doi.org/10.1063/1.4898075.
[9] W. Li, Y. Yang, J. K. Weber, G. Zhang, and R. Zhou, "Tunable, Strain-Controlled Nanoporous MoS_2 Filter for Water Desalination," ACS Nano **10**, 1829–1835 (2016).
[10] M. H. Köhler, J. R. Bordin, and M. C. Barbosa, "2D Nanoporous Membrane for Cation Removal from Water: Effects of Ionic Valence, Membrane Hydrophobicity, and Pore Size," The Journal of Chemical Physics **148**, 222804 (2018).
[11] J. Kou, J. Yao, L. Wu, X. Zhou, H. Lu, F. Wu, and J. Fan, "Nanoporous Two-Dimensional MoS_2 Membranes for Fast Saline Solution Purification," Physical Chemistry Chemical Physics **18**, 22210–22216 (2016).
[12] D. Cohen-Tanugi and J. C. Grossman, "Water desalination across nanoporous graphene," Nano Letters **12**, 3602–3608 (2012), pMID: 22668008, https://doi.org/10.1021/nl3012853.
[13] M. Akhavan, J. Schofield, and S. Jalili, "Water transport and desalination through double-layer graphyne membranes," Physical Chemistry Chemical Physics **20**, 13607–13615 (2018).
[14] D. Konatham, J. Yu, T. A. Ho, and A. Striolo, "Simulation insights for graphene-based water desalination membranes," Langmuir **29**, 11884–11897 (2013), pMID: 23848277, https://doi.org/10.1021/la4018695.
[15] D. Cohen-Tanugi, L.-C. Lin, and J. C. Grossman, "Multilayer nanoporous graphene membranes for water desalination," Nano Letters **16**, 1027–1033 (2016), pMID: 26806020, https://doi.org/10.1021/acs.nanolett.5b04089.
[16] M. Heiranian, A. B. Farimani, and N. R. Aluru, "Water desalination with a single-layer mos2 nanopore," Nature Communications **6**, 8616 (2015).
[17] Z. Cao, V. Liu, and A. Barati Farimani, "Why is single-layer mos2 a more energy efficient membrane for water desalination?" ACS Energy Letters **5**, 2217–2222 (2020), https://doi.org/10.1021/acsenergylett.0c00923.
[18] J. P. K. Abal, J. R. Bordin, and M. C. Barbosa, "Salt parameterization can drastically affect the results from classical atomistic simulations of water desalination by mos2 nanopores," Phys. Chem. Chem. Phys. **22**, 11053–11061 (2020).
[19] D. Cohen-Tanugi and J. C. Grossman, "Water permeability of nanoporous graphene at realistic pressures for reverse osmosis desalination," The Journal of Chemical Physics **141**, 074704 (2014), https://doi.org/10.1063/1.4892638.
[20] D. Jang, J.-C. Idrobo, T. Laoui, and R. Karnik, "Water and solute transport governed by tunable pore size distributions in nanoporous graphene membranes," ACS Nano **11**, 10042–10052 (2017), pMID: 28994572, https://doi.org/10.1021/acsnano.7b04299.
[21] Z. Wang and B. Mi, "Environmental applications of 2d molybdenum disulfide (mos2) nanosheets," Environmental Science & Technology **51**, 8229–8244 (2017), pMID: 28661657, https://doi.org/10.1021/acs.est.7b01466.
[22] H. Li, T.-J. Ko, M. Lee, H.-S. Chung, S. S. Han, K. H. Oh, A. Sadmani, H. Kang, and Y. Jung, "Experimental Realization of Few Layer Two-Dimensional MoS_2 Membranes of Near Atomic Thickness for High Efficiency Water Desalination," Nano Letters **19**, 5194–5204 (2019).
[23] Z. Wang, Q. Tu, S. Zheng, J. J. Urban, S. Li, and B. Mi, "Understanding the Aqueous Stability and Filtration Capability of MoS_2 Membranes," Nano Letters **17**, 7289–7298 (2017).
[24] W. Hirunpinyopas, E. Prestat, S. D. Worrall, S. J. Haigh, R. A. W. Dryfe, and M. A. Bissett, "Desalination and nanofiltration through functionalized laminar mos_2 membranes," ACS Nano **11**, 11082–11090 (2017), pMID: 29019650, https://doi.org/10.1021/acsnano.7b05124.
[25] C. Liu, Y. Jin, and Z. Li, "Water transport through graphene and mos2 nanopores," Journal of Applied Physics **126**, 024901 (2019), https://doi.org/10.1063/1.5104309.
[26] K. Kwac, I. Kim, T. A. Pascal, W. A. Goddard, H. G. Park, and Y. Jung, "Multilayer two-dimensional water structure confined in mos2," The Journal of Physical Chemistry C **121**, 16021–16028 (2017), https://doi.org/10.1021/acs.jpcc.7b05153.
[27] M. E. Suk and N. R. Aluru, "Molecular and continuum hydrodynamics in graphene nanopores," RSC Adv. **3**, 9365–9372 (2013).
[28] S. K. Kannam, P. J. Daivis, and B. Todd, "Modeling slip and flow enhancement of water in carbon nanotubes," MRS Bulletin **42**, 283–288 (2017).
[29] P. Sahu and S. M. Ali, "Breakdown of continuum model for water transport and desalination through ultrathin graphene nanopores: insights from molecular dynamics simulations," Phys. Chem. Chem. Phys. **21**, 21389–21406 (2019).
[30] K. H. Jensen, A. X. C. N. Valente, and H. A. Stone, "Flow rate through microfilters: Influence of the pore size distribution, hydrodynamic interactions, wall slip, and inertia," Physics of Fluids **26**, 052004 (2014), https://doi.org/10.1063/1.4876937.
[31] D. Cohen-Tanugi, R. K. McGovern, S. H. Dave, J. H. Lienhard, and J. C. Grossman, "Quantifying the potential of ultra-permeable membranes for water desalination," Energy Environ. Sci. **7**, 1134–1141 (2014).
[32] M. R. Hasan and B. Kim, "Molecular transportation phenomena of simple liquids through a nanoporous graphene membrane," Phys. Rev. E **102**,

033110 (2020).
[33]R. Fuentes-Azcatl and M. C. Barbosa, "Sodium chloride, nacl/e: New force field," The Journal of Physical Chemistry B **120**, 2460–2470 (2016), pMID: 26890321, https://doi.org/10.1021/acs.jpcb.5b12584.
[34]R. Fuentes-Azcatl and M. C. Barbosa, "Thermodynamic and dynamic anomalous behavior in the tip4p/e water model," Physica A: Statistical Mechanics and its Applications **444**, 86 – 94 (2016).
[35]E. S. Kadantsev and P. Hawrylak, "Electronic structure of a single mos2 monolayer," Solid State Communications **152**, 909 – 913 (2012).
[36]G. Hummer, J. C. Rasaiah, and J. P. Noworyta, "Water conduction through the hydrophobic channel of a carbon nanotube," Nature **414**, 188–190 (2001).
[37]S. Plimpton, "Fast parallel algorithms for short-range molecular dynamics," Journal of Computational Physics **117**, 1 – 19 (1995).
[38]E. M. V. Hoek, A. S. Kim, and M. Elimelech, "Influence of crossflow membrane filter geometry and shear rate on colloidal fouling in reverse osmosis and nanofiltration separations," Environmental Engineering Science **19**, 357–372 (2002), https://doi.org/10.1089/109287502320963364.
[39]M. Yang, X. Yang, Q. Wang, K. Wang, X. Fan, W. Liu, X. Liu, J. Liu, and J. Huang, "Anomalous effects of water flow through charged nanochannel membranes," RSC Adv. **4**, 26729–26737 (2014).
[40]L. Hao, J. Su, and H. Guo, "Water permeation through a charged channel," The Journal of Physical Chemistry B **117**, 7685–7694 (2013), pMID: 23742655, https://doi.org/10.1021/jp400578u.
[41]Z. Huang, Y. Zhang, T. Hayashida, Z. Ji, Y. He, M. Tsutsui, X. S. Miao, and M. Taniguchi, "The impact of membrane surface charges on the ion transport in mos2 nanopore power generators," Applied Physics Letters **111**, 263104 (2017), https://doi.org/10.1063/1.5003695.
[42]H. Gao, Q. Shi, D. Rao, Y. Zhang, J. Su, Y. Liu, Y. Wang, K. Deng, and R. Lu, "Rational design and strain engineering of nanoporous boron nitride nanosheet membranes for water desalination," The Journal of Physical Chemistry C **121**, 22105–22113 (2017), https://doi.org/10.1021/acs.jpcc.7b06480.
[43]J.-W. Jiang, "Graphene versus mos2: A short review," Frontiers of Physics **10**, 287–302 (2015).

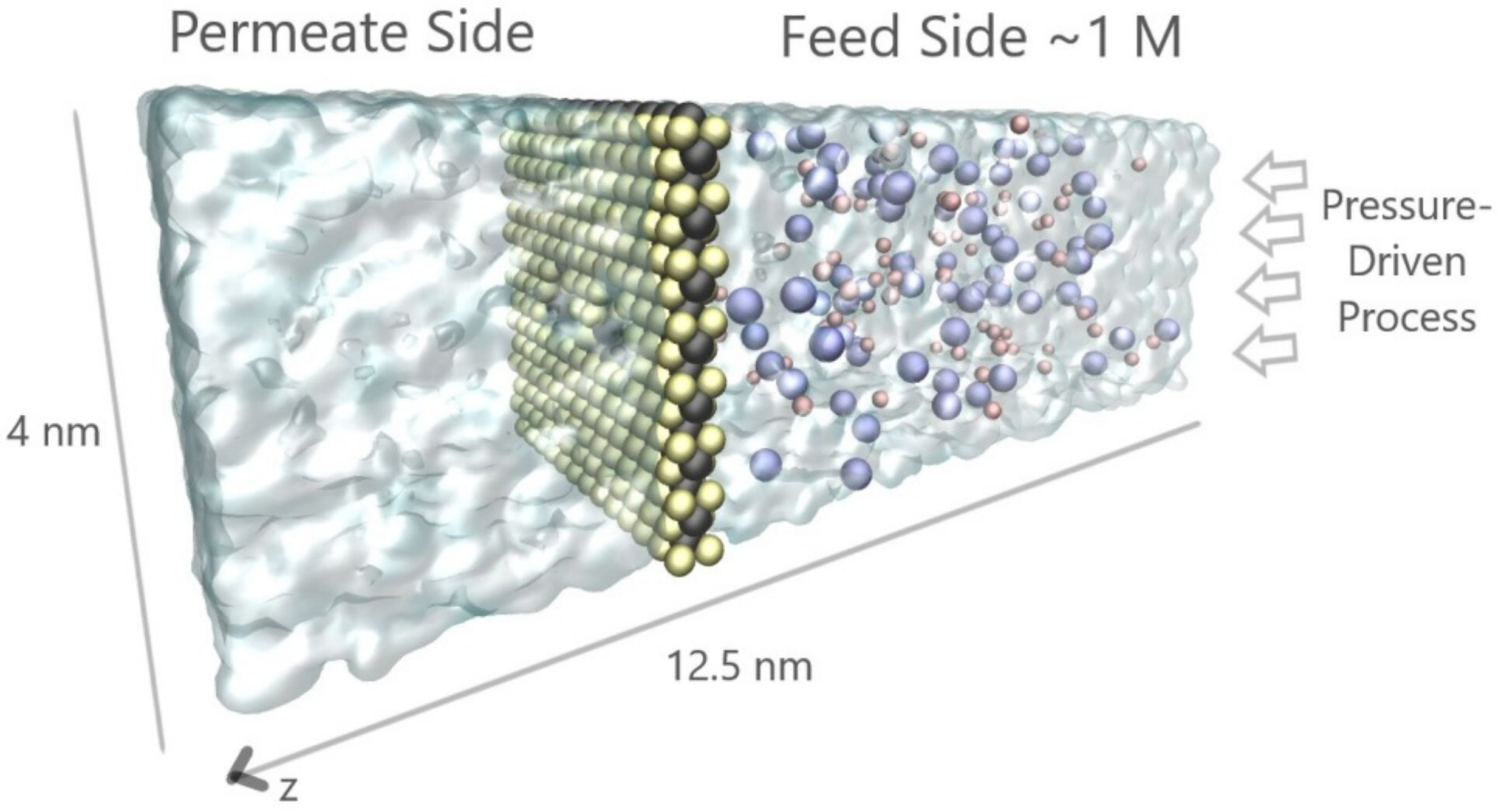
Permeate Side
Feed Side ~1 M
Pressure-
Driven
Process
4 nm
12.5 nm
z

4 nm
d = 0.97 nm {
4 nm
~ 1.3 nm
~ 1.6 nm
~ 1.9 nm
~ 1.6 nm
~ 2.3 nm
~ 1.3 nm
~ 1.3 nm

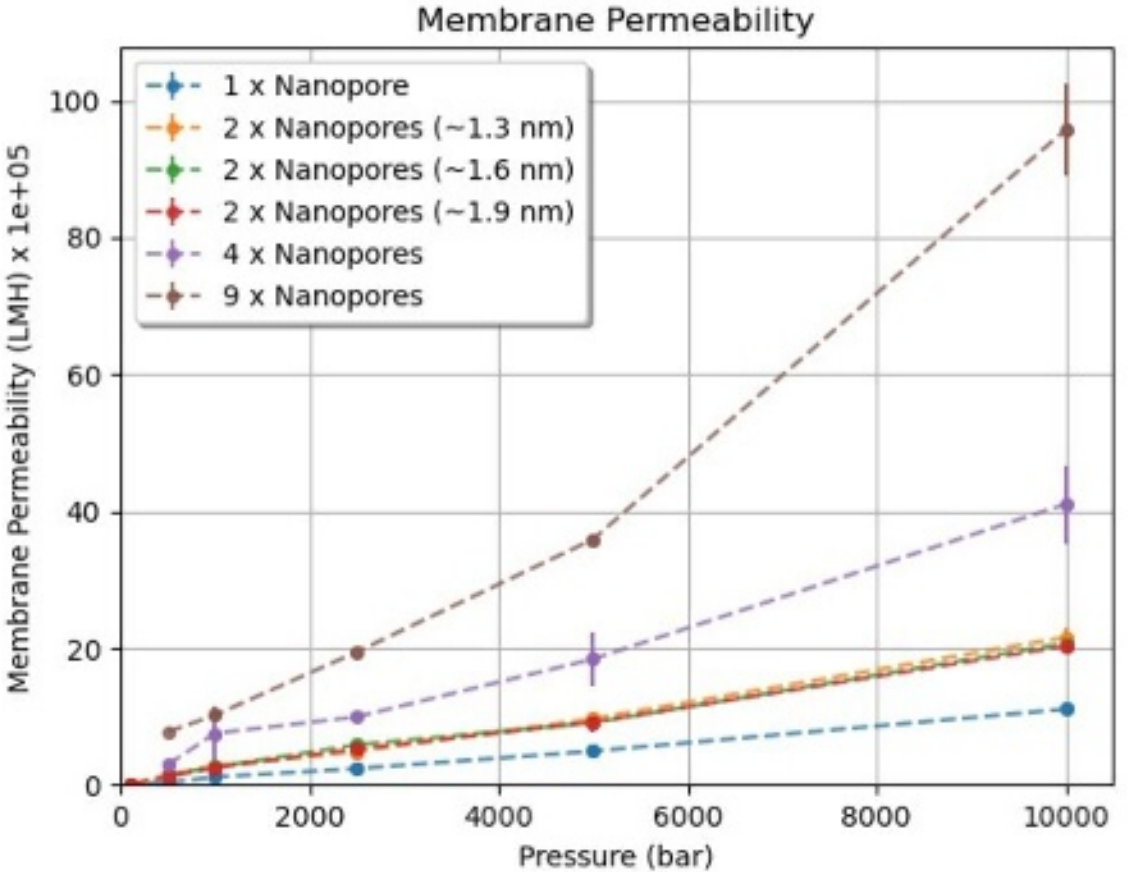
Membrane Permeability
1 x Nanopore
2 x Nanopores (~1.3 nm)
2 x Nanopores (~1.6 nm)
2 x Nanopores (~1.9 nm)
4 x Nanopores
9 x Nanopores
Membrane Permeability (LMH) x 1e+05
Pressure (bar)
0
20
40
60
80
100
0
2000
4000
6000
8000
10000

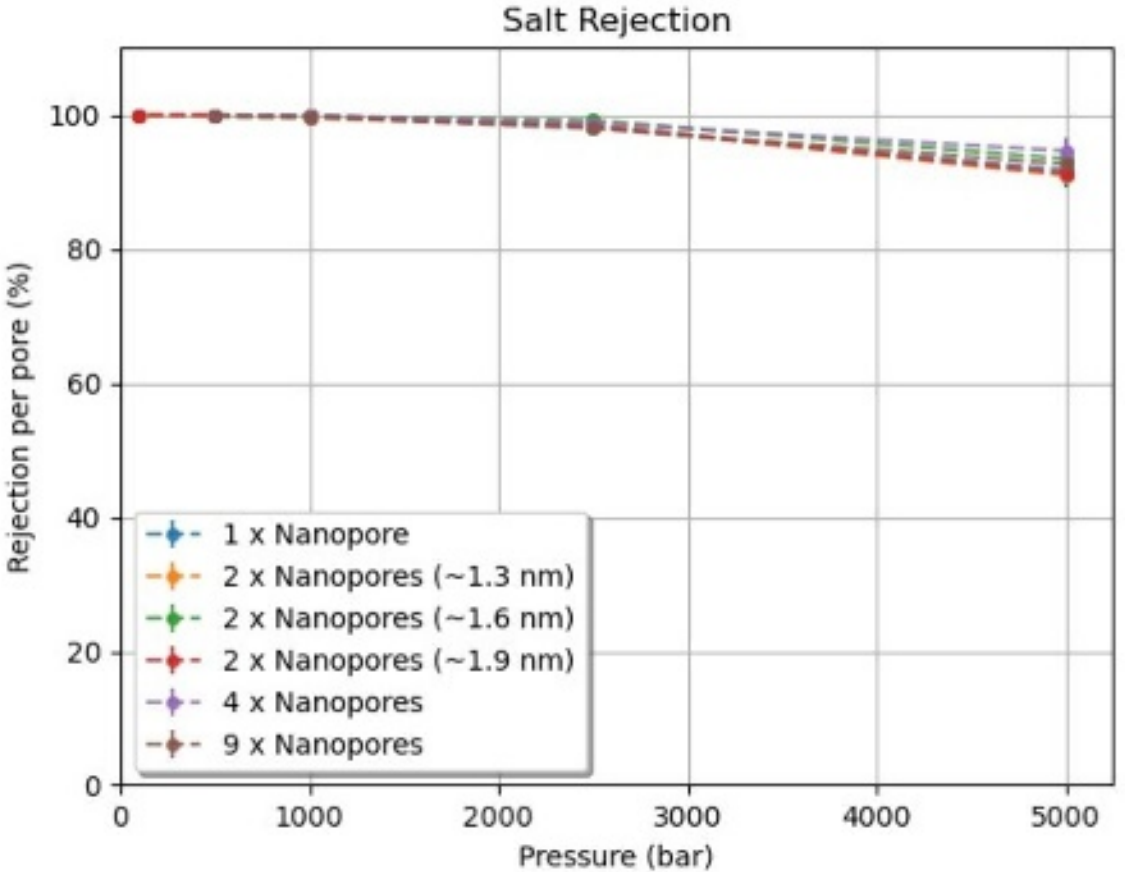
Salt Rejection
Rejection per pore (%)
Pressure (bar)
0
20
40
60
80
100
0
1000
2000
3000
4000
5000
1 x Nanopore
2 x Nanopores (~1.3 nm)
2 x Nanopores (~1.6 nm)
2 x Nanopores (~1.9 nm)
4 x Nanopores
9 x Nanopores

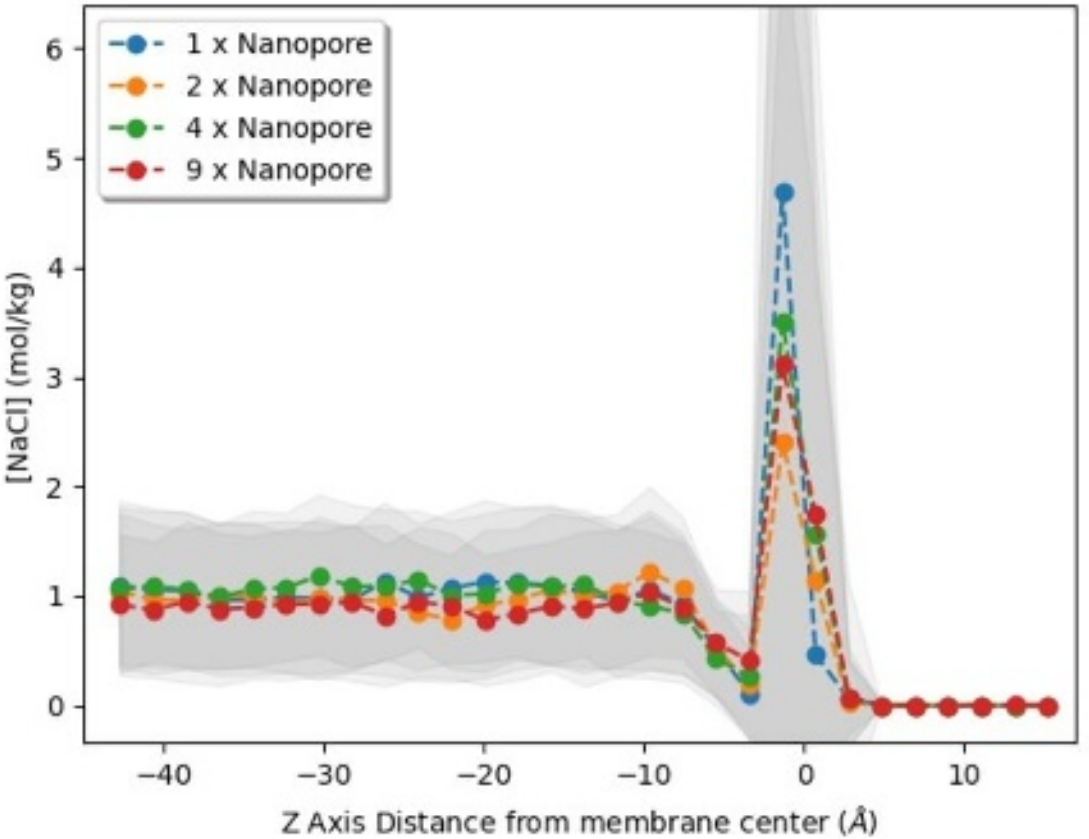
1 x Nanopore
2 x Nanopore
4 x Nanopore
9 x Nanopore
[NaCl] (mol/kg)
0
1
2
3
4
5
6
−40
−30
−20
−10
0
10
Z Axis Distance from membrane center (Å)

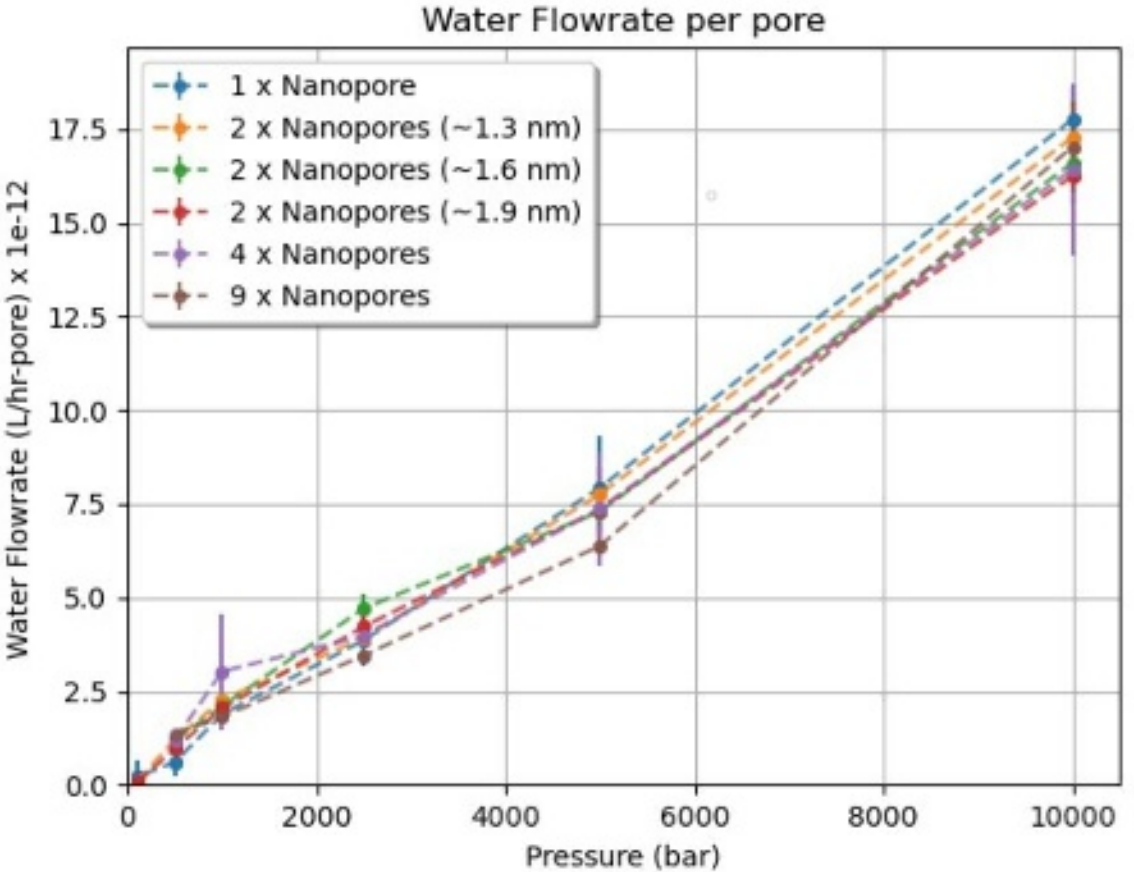
Water Flowrate per pore
1 x Nanopore
2 x Nanopores (~1.3 nm)
2 x Nanopores (~1.6 nm)
2 x Nanopores (~1.9 nm)
4 x Nanopores
9 x Nanopores
Water Flowrate (L/hr-pore) x 1e-12
0.0
2.5
5.0
7.5
10.0
12.5
15.0
17.5
0
2000
4000
6000
8000
10000
Pressure (bar)

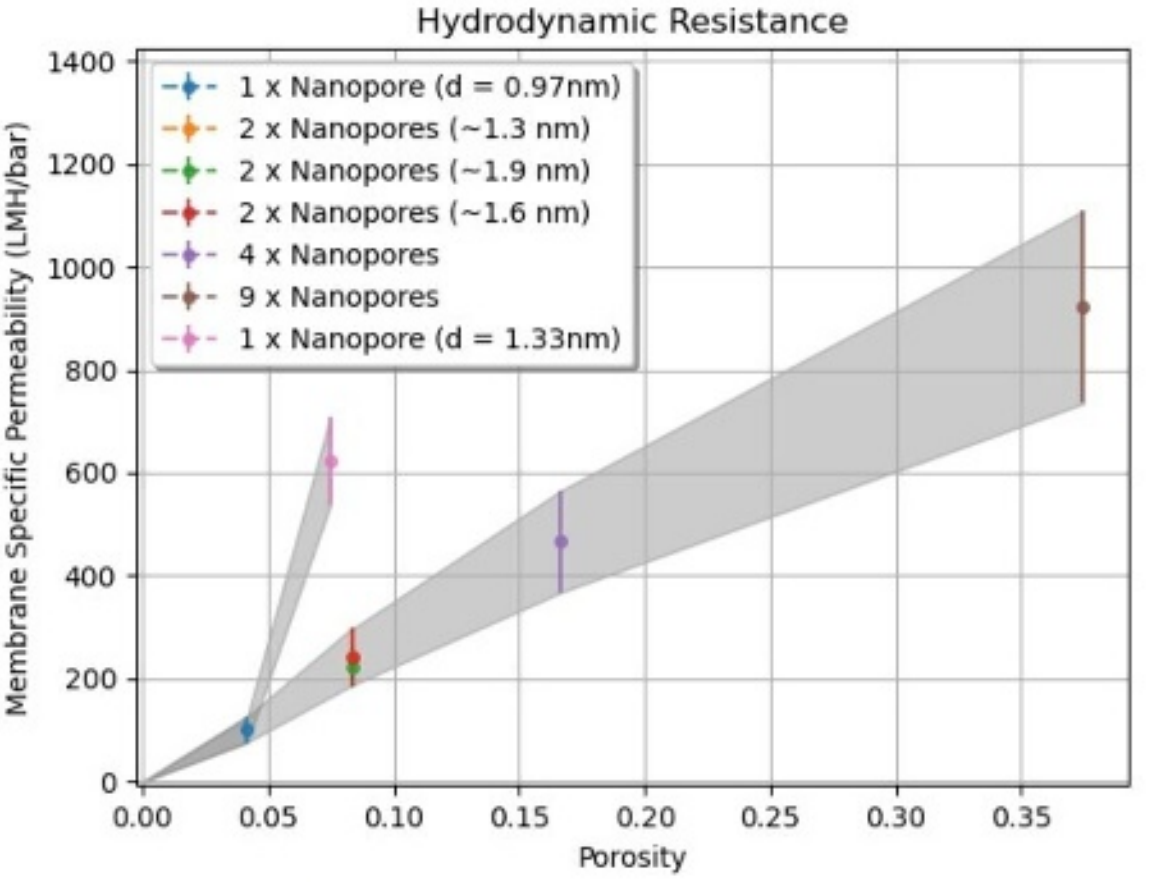

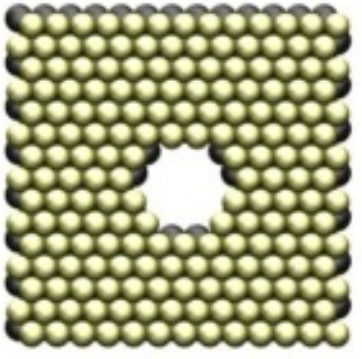

1 x Nanopore (d = 1.33nm)

Region 2

Region 3

Region 1

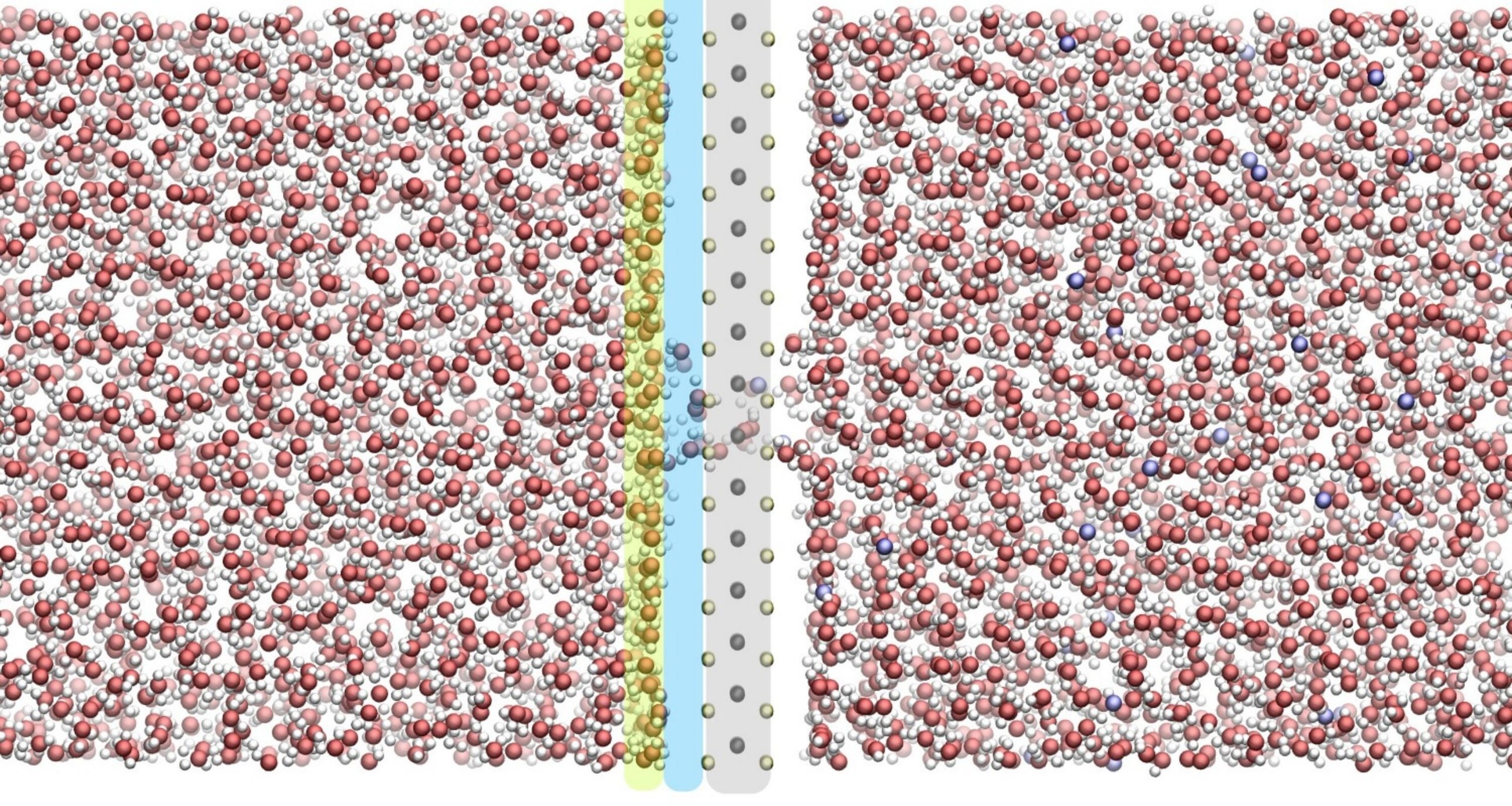

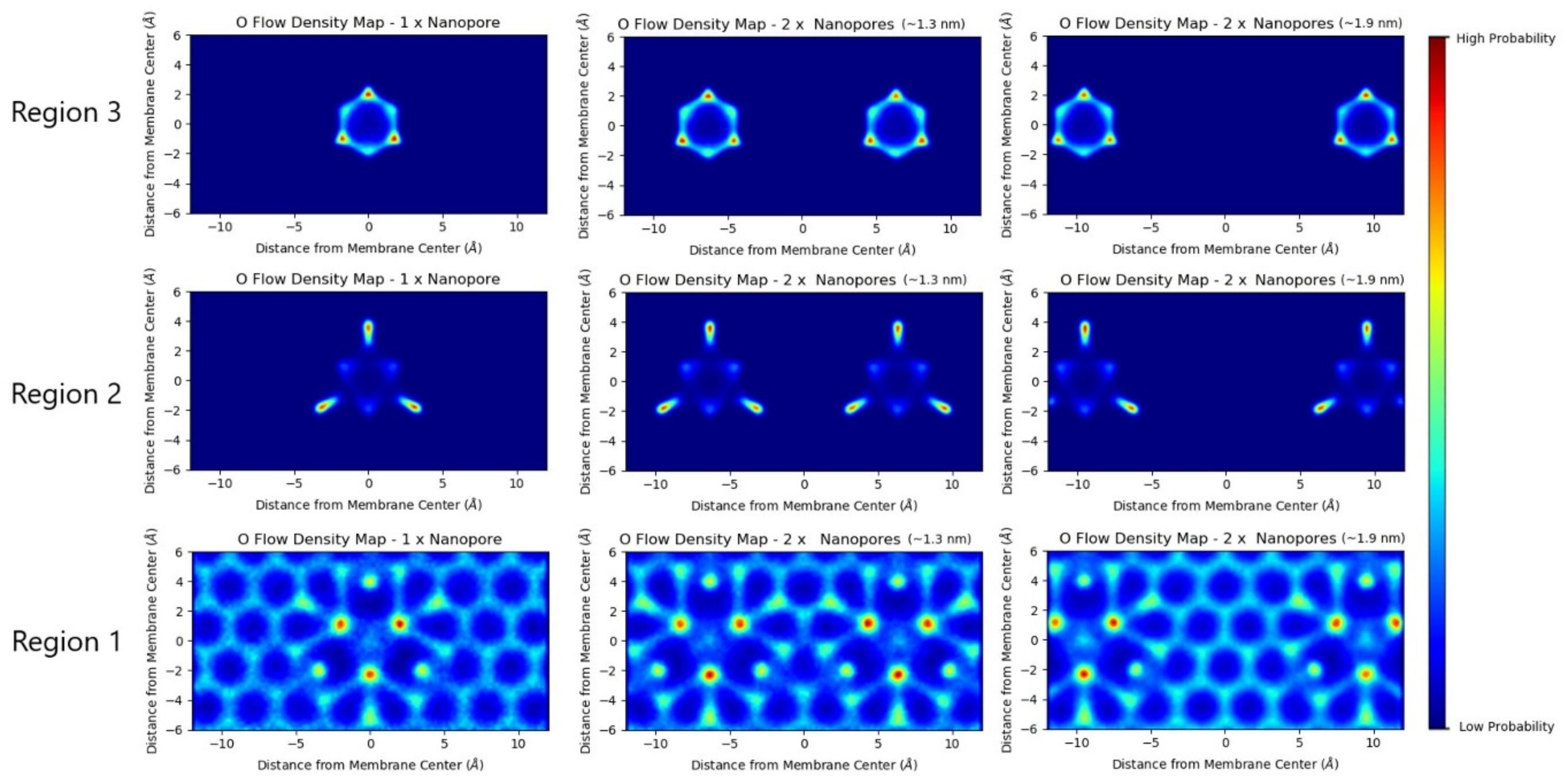
Region 3
Region 2
Region 1
O Flow Density Map - 1 x Nanopore
O Flow Density Map - 2 x Nanopores (~1.3 nm)
O Flow Density Map - 2 x Nanopores (~1.9 nm)
Distance from Membrane Center (Å)
High Probability
Low Probability

a)

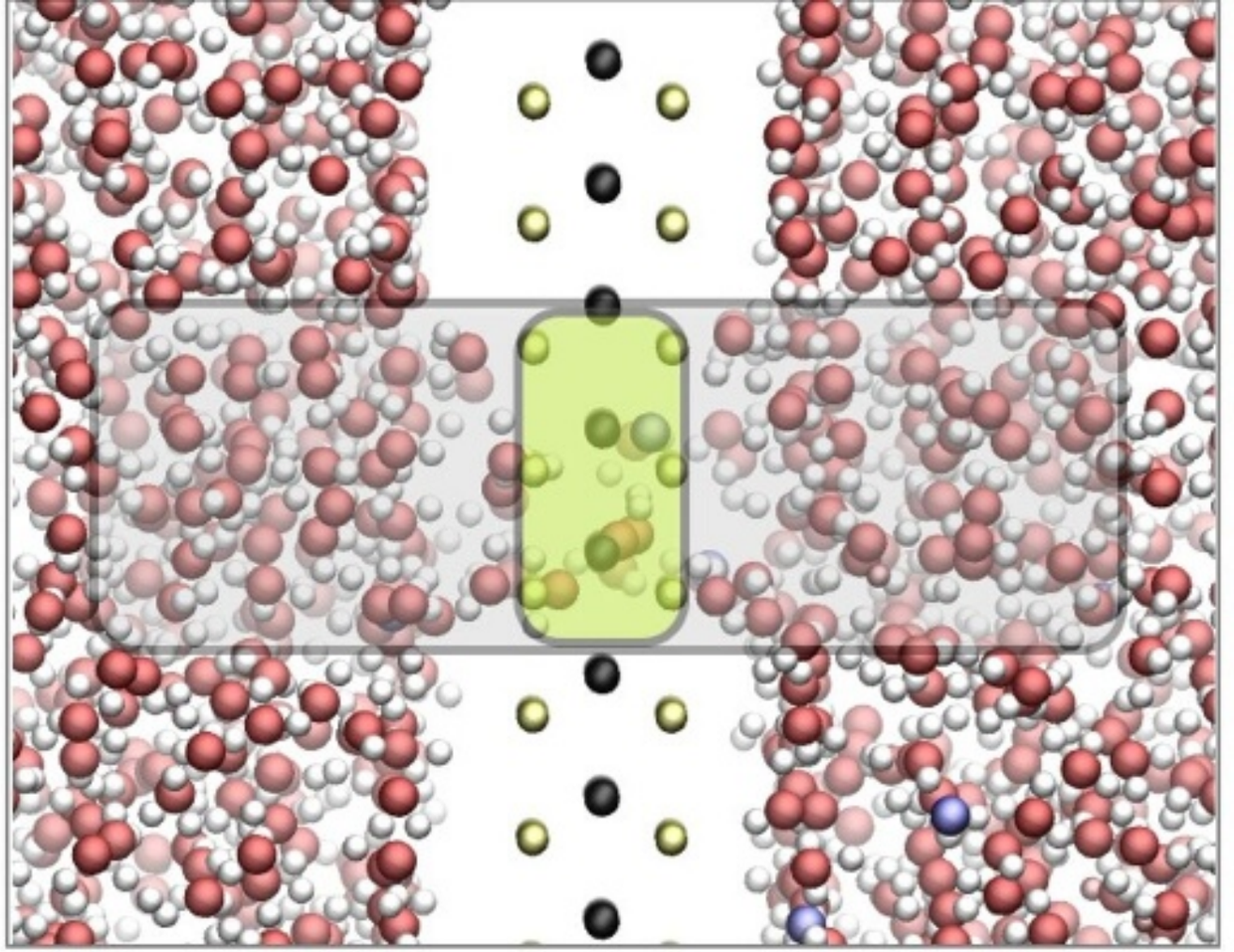

Nanopore Region

Entrance and Nanopore Region

b)

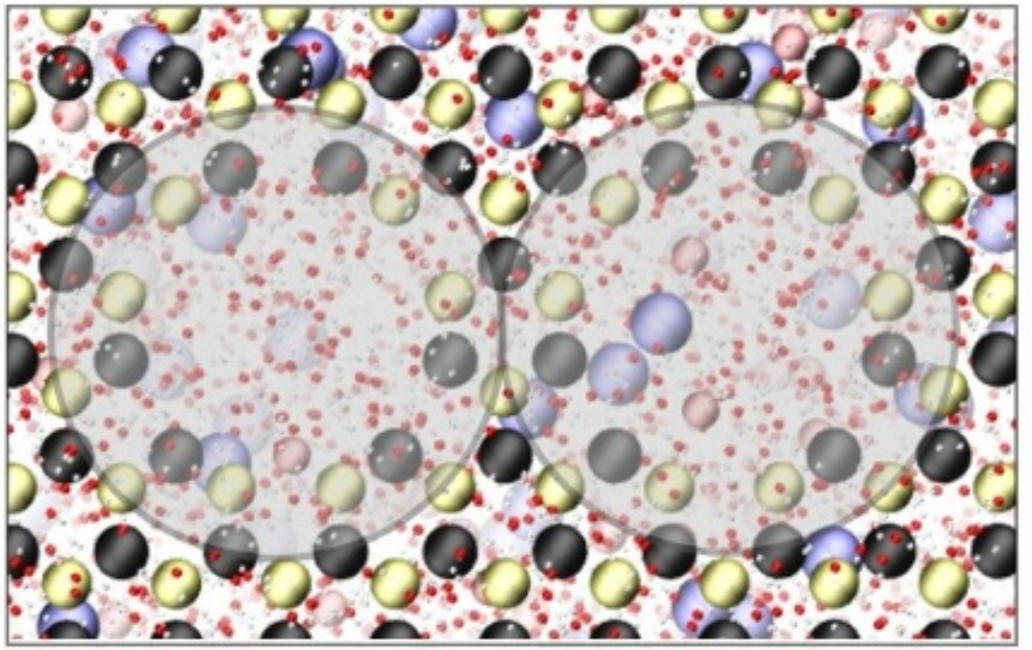

Molybdenum (Mo)

Sulfur (S)

Sodium (Na)

Chloride (Cl)

Water (H_2O)

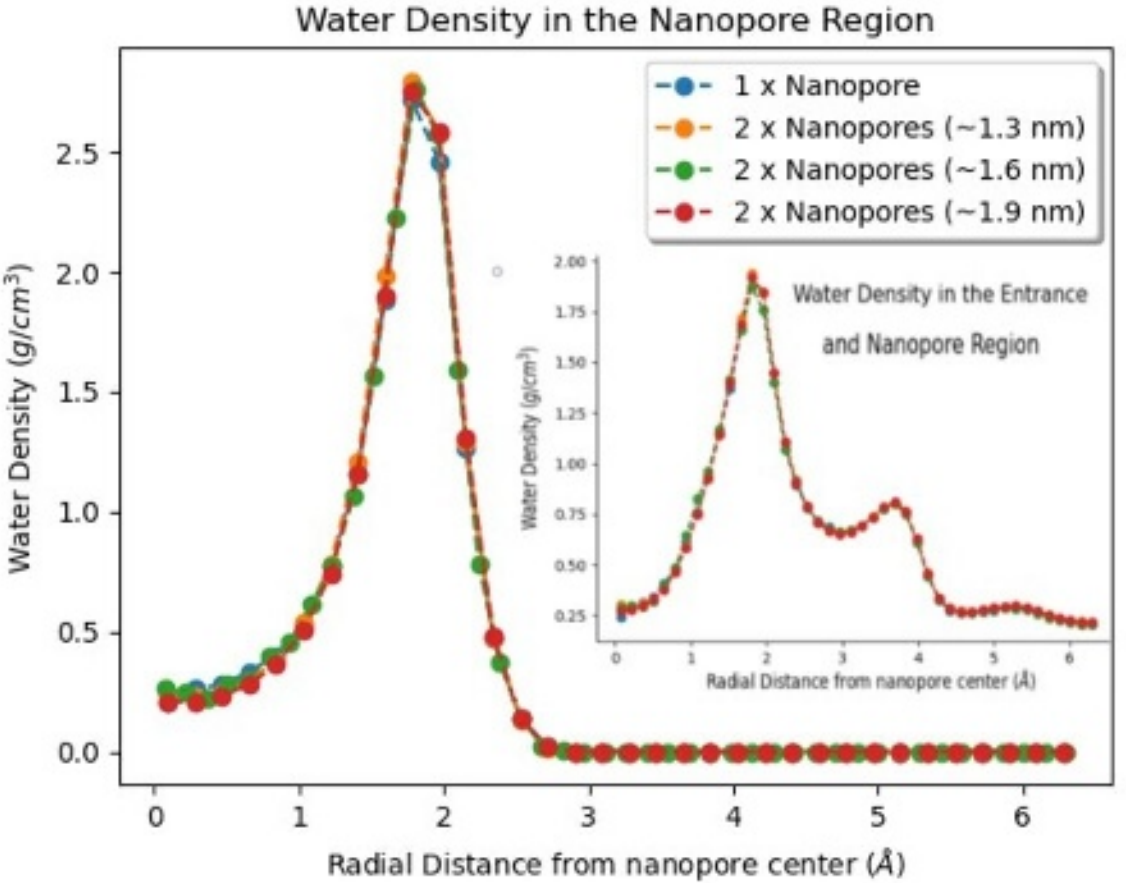
Water Density in the Nanopore Region
1 x Nanopore
2 x Nanopores (~1.3 nm)
2 x Nanopores (~1.6 nm)
2 x Nanopores (~1.9 nm)
Water Density (g/cm³)
Radial Distance from nanopore center (Å)
Water Density in the Entrance and Nanopore Region
Water Density (g/cm³)
Radial Distance from nanopore center (Å)

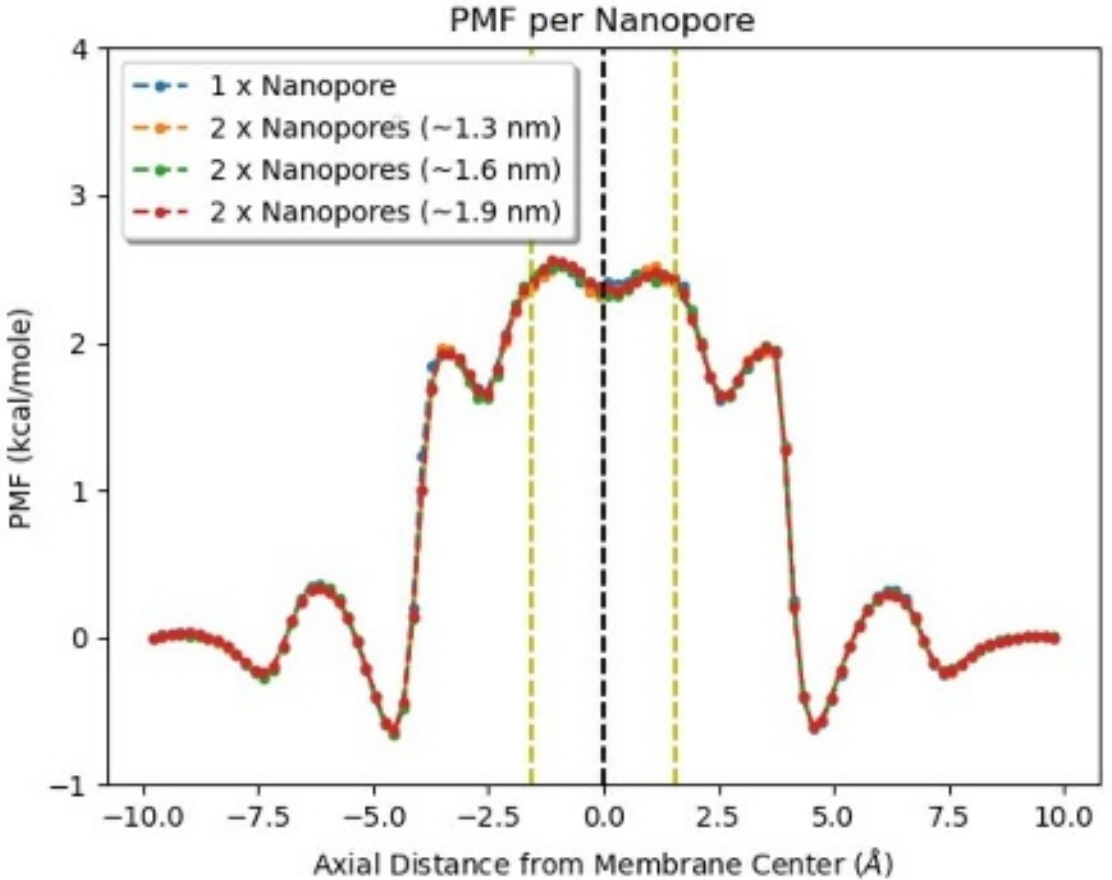
PMF per Nanopore
1 x Nanopore
2 x Nanopores (~1.3 nm)
2 x Nanopores (~1.6 nm)
2 x Nanopores (~1.9 nm)
PMF (kcal/mole)
4
3
2
1
0
−1
−10.0
−7.5
−5.0
−2.5
0.0
2.5
5.0
7.5
10.0
Axial Distance from Membrane Center (Å)